

# Onset of Fast Reconnection in Hall Magnetohydrodynamics Mediated by the Plasmoid Instability

Yi-Min Huang,\* A. Bhattacharjee, and Brian P. Sullivan

*Center for Integrated Computation and Analysis of Reconnection and Turbulence and  
Center for Magnetic Self-Organization in Laboratory and Astrophysical Plasmas,  
University of New Hampshire, Durham, NH 03824*

## Abstract

The role of a super-Alfvénic plasmoid instability in the onset of fast reconnection is studied by means of the largest Hall magnetohydrodynamics simulations to date, with system sizes up to  $10^4$  ion skin depths ( $d_i$ ). It is demonstrated that the plasmoid instability can facilitate the onset of rapid Hall reconnection, in a regime where the onset would otherwise be inaccessible because the Sweet-Parker width is significantly above  $d_i$ . However, the topology of Hall reconnection is not inevitably a single stable X-point. There exists an intermediate regime where the single X-point topology itself exhibits instability, causing the system to alternate between a single X-point geometry and an extended current sheet with multiple X-points produced by the plasmoid instability.

---

\*Electronic address: yimin.huang@unh.edu

## I. INTRODUCTION

Magnetic reconnection is thought to be the underlying mechanism that powers explosive events such as flares, substorms, and sawtooth crashes in fusion plasmas[1]. Such events commonly feature impulsive onset, whereby the system exhibits a sudden increase in the reconnection rate[2]. In classic Sweet-Parker theory[3, 4], based on resistive magnetohydrodynamics (MHD), the reconnection site has the structure of a thin current sheet of length  $L$ , which is of the order of the system size, and a width  $\delta_{SP} \simeq L/\sqrt{S}$ , where the Lundquist number  $S$  is related to the length  $L$ , the Alfvén speed  $V_A$ , and the resistivity  $\eta$  by the relation  $S \equiv LV_A/\eta$ . The plasma outflow speed from the reconnection site is approximately  $V_A$ , and the inflow speed, which is a measure of the reconnection rate, is approximately  $V_A/S^{1/2}$  under quasi-steady conditions. In most plasmas of interest, the Lundquist numbers are very high. Consequently, the Sweet-Parker reconnection rates are usually several orders of magnitude too slow to account for the observed rate of energy release after onset. The strong dependence of the reconnection rate on  $S$  in the Sweet-Parker theory has led to a broad consensus that the solution to the onset problem for high- $S$  plasmas lies outside the domain of resistive MHD, and requires the inclusion of collisionless effects. In particular, for two-dimensional (2D) configurations without a guide field, a precise criterion has been proposed that accounts for a slow growth phase (identified as a Sweet-Parker phase in many cases of interest), followed by rapid onset caused by the Hall current, which is a signature of the decoupling of electron and ion motion at scales below the ion skin depth  $d_i$  [5–8]. (Here  $d_i = c/\omega_{pi}$ , where  $c$  is the speed of light and  $\omega_{pi}$  is the ion plasma frequency.) The criterion predicts that when  $\delta_{SP} < d_i$ , the system will spontaneously make a transition to a rapid reconnection phase, with an inflow velocity  $\sim 0.1V_A$ . This criterion has been tested extensively by numerical simulations[5–8] as well as controlled experiments[9].

The recent discovery of a linear, super-Alfvénic plasmoid instability[10] in high- $S$  plasmas raises qualitatively new questions for the criterion stated above. It has long been known that the Sweet-Parker reconnection layer can become unstable to a secondary tearing instability. However, only recently has a precise linear study shown that the linear growth rate  $\gamma$  of the instability scales as  $\gamma \sim S^{1/4}(V_A/L)$ . The positive exponent of  $S$  yields high growth rates for high  $S$  plasmas, whereas most resistive instabilities scale with  $S$  to some negative fractional power. This seemingly counterintuitive result can actually be deduced from the dispersion

relation for classical tearing modes[11] with one crucial new insight: the Sweet-Parker layer supports an increasingly singular current sheet as  $S \rightarrow \infty$ . [12] Furthermore, even within the framework of resistive MHD, this linear instability leads to a nonlinear regime where the reconnection rate becomes nearly independent of  $S$ , with an inflow velocity  $\sim 10^{-2}V_A$ . [12, 13] The original Sweet-Parker current sheet breaks up into a chain of plasmoids and a sequence of shorter but thinner current sheets, with widths much smaller than  $\delta_{SP}$ . [12, 14, 15]

The presence of the plasmoid instability in high- $S$  systems uncovers a deep flaw in the Sweet-Parker model, and raises questions about the conventional scenario of the onset of Hall reconnection. The following important questions of principle arise: Can the plasmoid instability trigger the onset of Hall MHD reconnection in systems that do not meet the original criterion  $\delta_{SP} < d_i$  for onset? What is the interplay between the plasmoid instability and the Hall current as secondary current sheets cascade down to widths at the  $d_i$  scale? Does the onset of Hall reconnection inevitably lead to a Hall current dominated regime in which all plasmoids are expelled?[16] Can Hall MHD realize current sheet geometries qualitatively similar to those seen in fully kinetic simulations, where new plasmoids are constantly generated?[14] In this paper, we address these questions by means of the largest two-dimensional Hall MHD reconnection simulations ever carried out, with the ratio  $L/d_i$  ranging from  $2.5 \times 10^3$  to  $1.0 \times 10^4$ . The key results are: (1) The plasmoid instability can trigger the onset of Hall MHD reconnection in systems that do not meet the criterion  $\delta_{SP} < d_i$  for onset. (2) The topology of Hall MHD reconnection is not inevitably a single stable X-point, although the single X-point topology is one possible realization. (3) There exists an intermediate regime where the single X-point topology itself exhibits instability, causing the system to alternate between a single X-point and an extended current sheet with multiple X-points produced by the plasmoid instability. The latter raises the interesting possibility for the first time that Hall MHD simulations have the potential to realize extended current sheets that that have geometrical features similar to those seen in fully kinetic simulations.[14]

## II. NUMERICAL MODEL

Our simulations are based on resistive Hall MHD equations. These equations in normalized form are:

$$\partial_t \rho + \nabla \cdot (\rho \mathbf{u}) = 0, \quad (1)$$

$$\partial_t(\rho\mathbf{u}) + \nabla \cdot (\rho\mathbf{u}\mathbf{u}) = -\nabla p + \mathbf{J} \times \mathbf{B} + \epsilon\mathbf{f}(\mathbf{x}, t), \quad (2)$$

$$\partial_t\mathbf{B} = -\nabla \times \mathbf{E}, \quad (3)$$

$$\mathbf{E} = -\mathbf{u} \times \mathbf{B} + d_i \frac{\mathbf{J} \times \mathbf{B} - \nabla p_e}{\rho} + \eta\mathbf{J}, \quad (4)$$

where  $\rho$  is the plasma density,  $\mathbf{u}$  is the ion velocity,  $p$  is the total pressure,  $p_e$  is the electron pressure,  $\mathbf{B}$  is the magnetic field,  $\mathbf{E}$  is the electric field,  $\mathbf{J} = \nabla \times \mathbf{B}$  is the electric current density,  $\eta$  is the resistivity, and  $d_i$  is the ion skin depth. Isothermal equation of states are assumed, *i.e.*  $p_e = p_i = \rho T$ , where  $p_i$  is ion pressure, and  $T$  is a constant temperature. The total pressure is  $p = p_e + p_i = 2\rho T$ . Electron inertia terms are neglected in the generalized Ohm's law, Eq. (4). The electron pressure term  $-d_i\nabla p_e/\rho$  has been omitted in this study, because it does not contribute to the dynamics after taking the curl of  $\mathbf{E}$  in Eq. (3), due to the isothermal equation of state. A weak random forcing term  $\epsilon\mathbf{f}$  is added to the ion momentum equation, as was done in a previous study.[13] The normalizations of Eqs. (1) – (4) are based on constant reference values of the density  $n_0$ , and the magnetic field  $B_0$ . Lengths are normalized to the system size  $L$ , and time is normalized to the global Alfvén time  $t_A = L/V_A$ , where  $V_A = B_0/\sqrt{4\pi n_0 m_i}$  and  $m_i$  is the ion mass. The normalizations of physical variables are given by (normalized  $\rightarrow$  physical units):  $\rho \rightarrow \rho/n_0 m_i$ ,  $\mathbf{B} \rightarrow \mathbf{B}/B_0$ ,  $\mathbf{E} \rightarrow c\mathbf{E}/B_0 V_A$ ,  $\mathbf{u} \rightarrow \mathbf{u}/V_A$ ,  $p \rightarrow p/n_0 m_i V_A^2$ ,  $\mathbf{J} \rightarrow \mathbf{J}/(B_0 c/4\pi L)$ , and  $d_i \rightarrow d_i/L \equiv \sqrt{m_i c^2/4\pi n_0 e^2}/L$ . In 2D simulations, the magnetic field is expressed in terms of the flux function  $\psi$  and the out-of-plane component  $B_y$  as  $\mathbf{B} = \nabla\psi \times \hat{\mathbf{y}} + B_y\hat{\mathbf{y}}$ . The variables  $\psi$  and  $B_y$  are stepped in the code. The governing equations are numerically solved with a massively parallel code HMHD, which is a two-fluid extension to the resistive MHD code used in previous studies.[12, 13] The numerical algorithm [17] approximates spatial derivatives by finite differences with a five-point stencil in each direction. The time-stepping scheme can be chosen from several options including a second-order accurate trapezoidal leapfrog method and various strong stability preserving Runge–Kutta methods.[18, 19] We employ the second-order accurate trapezoidal leapfrog method in this study. HMHD has the capability of nonuniform meshes that allows better resolution of the reconnection layer.

We employ the same simulation setup of two coalescing magnetic islands as in a previous study[13]. The 2D simulation box is the domain  $(x, z) \in [-1/2, 1/2] \times [-1/2, 1/2]$ . In normalized units, the initial magnetic field is given by  $\mathbf{B}_0 = \nabla\psi_0 \times \hat{\mathbf{y}}$ , where  $\psi_0 =$

$\tanh(z/h) \cos(\pi x) \sin(2\pi z)/2\pi$ . The parameter  $h$ , which is set to 0.01 for all simulations, determines the initial current layer width. The initial plasma density  $\rho$  is approximately 1, and the plasma temperature  $T$  is 3. The density profile has a weak nonuniformity such that the initial condition is approximately force balanced. The initial peak magnetic field and Alfvén speed are both approximately unity. The plasma beta  $\beta \equiv p/B^2 = 2\rho T/B^2$  is greater than 6. Perfectly conducting and free slipping boundary conditions are imposed along both  $x$  and  $z$  directions. Specifically, we have  $\psi = 0$ ,  $\mathbf{u} \cdot \hat{\mathbf{n}} = 0$ ,  $\hat{\mathbf{n}} \cdot \nabla(\hat{\mathbf{n}} \times \mathbf{u}) = 0$ ,  $\hat{\mathbf{n}} \cdot \nabla\rho = 0$ , and  $B_y = 0$  on the boundaries (here  $\hat{\mathbf{n}}$  is the unit normal vector to the boundary). Only half of the domain ( $z \geq 0$ ) is simulated, and solutions in the other half are inferred by symmetries. The computational mesh consists of  $6400 \times 1024$  grid points. The grid points along  $z$  are strongly concentrated around  $z = 0$ , with the smallest grid size  $\Delta z = 1.4 \times 10^{-5}$ . The grid points along  $x$  are weakly nonuniform, with the smallest grid size  $\Delta x = 1.2 \times 10^{-4}$  at  $x = 0$ . For this system, the critical Lundquist number  $S_c$  for onset of the plasmoid instability is approximately  $4 \times 10^4$  in resistive MHD ( $d_i = 0$ ).[13]

When the Hall effect is included, the system is characterized by two important dimensionless parameters:  $S$  and  $L/d_i$ . The parameter space of  $S$  and  $L/d_i$  may be divided qualitatively into four regions, shown in Figure 1. The Hall reconnection regime is realized when the conventional criterion  $d_i > \delta_{SP}$  for onset of Hall reconnection is satisfied. Under this condition, we recover the standard results for the onset of Hall reconnection.[5–8] The Sweet-Parker reconnection regime is realized when neither the criterion for onset of Hall reconnection  $d_i > \delta_{SP}$  nor that for the plasmoid instability  $S > S_c$  are satisfied. In this regime, a stable, elongated Sweet-Parker current layer is formed. When the Lundquist number  $S$  exceeds the critical value  $S_c$  for onset of the plasmoid instability, two new possibilities emerge. If the secondary current sheets cascade down to widths at the  $d_i$  scale, we may expect onset of Hall reconnection. On the other hand, if the secondary current sheets never reach the  $d_i$  scale, the reconnection may proceed in a manner similar to that in resistive MHD. To delineate the border between these two regimes, an estimate for the widths of secondary current sheets is needed. In a previous resistive MHD study, we found that a good estimate for the average width of the secondary current sheets is obtained by requiring that they obey Sweet-Parker scaling, with a length that keeps them marginally stable. That gives an average width  $\delta \sim \delta_{SP}(S_c/S)^{1/2} \sim LS_c^{1/2}/S$ . [13] We denote the regime where  $\delta < d_i$  as “Hall reconnection triggered by plasmoids”, and the regime where  $\delta > d_i$  as

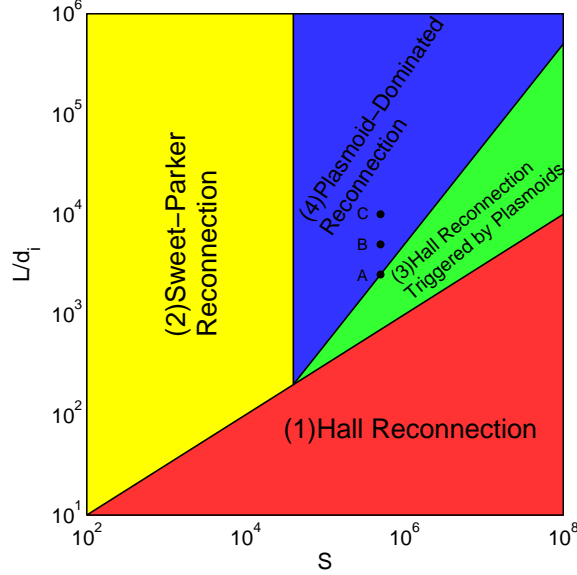


Figure 1: (Color online) The parameter space is divided into four regions. (1) Hall reconnection:  $d_i > \delta_{SP}$ . (2) Sweet-Parker reconnection:  $d_i < \delta_{SP}$  and  $S < S_c$ . (3) Hall reconnection triggered by plasmoids:  $\delta_{SP}(S_c/S)^{1/2} < d_i < \delta_{SP}$ . (4) Plasmoid-dominated reconnection:  $S > S_c$  and  $\delta_{SP}(S_c/S)^{1/2} > d_i$ . The dots denote the parameters for three different runs. All three runs have  $S = 5 \times 10^5$ . The parameter  $L/d_i$  is  $2.5 \times 10^3$  for Run A,  $5 \times 10^3$  for Run B, and  $10^4$  for Run C, respectively. A fourth run, Run D, from a previous resistive MHD study[13], corresponds to  $L/d_i \rightarrow \infty$ , therefore is not shown.

“plasmoid-dominated reconnection” to characterize their different possible behaviors. Note that statistical deviations from the average width can and do occur.[13] As individual secondary current sheets can be significantly thinner than the average width, we expect the “Hall reconnection triggered by plasmoids” region to be larger than depicted in Figure 1. We caution that since high- $S$ , large-scale Hall MHD reconnection is largely unexplored, Figure 1 cannot be regarded as a complete picture because it includes ranges of parameter space where no simulations exist. Even the critical Lundquist number  $S_c$  and the secondary current sheet width  $\delta$  could be modified by the presence of the Hall effect. Furthermore, the criterion for onset  $\delta < d_i$  is only accurate up to a numerical factor of order unity. For these reasons, the delineation of different regimes in Figure 1 may not be very precise. Nonetheless, Figure 1 serves well in guiding the choice of simulation parameters where interesting physics may arise.

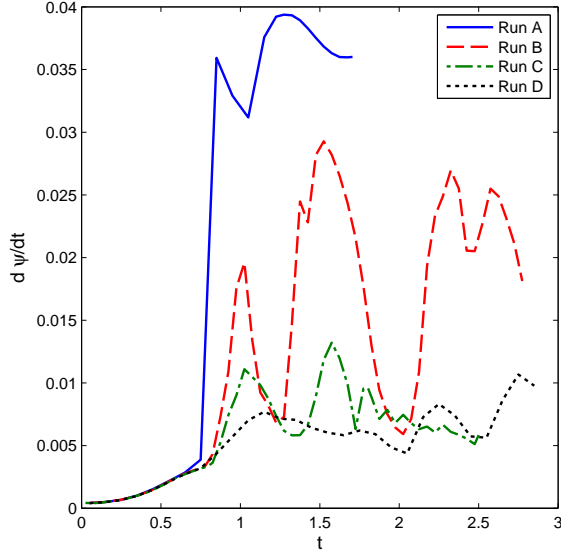


Figure 2: (Color online) The reconnection rate as a function of time, for four different runs.

The primary interest of this work is to explore the two new regimes where the plasmoid instability may play an important role. This study includes three new runs (Run A to C), with corresponding parameters marked on Figure 1. A fourth run, Run D, from a previous resistive MHD study[13], is included for comparison. We fix  $S = 5 \times 10^5$  for all runs. The parameter  $L/d_i$  is  $2.5 \times 10^3$  for Run A,  $5 \times 10^3$  for Run B, and  $10^4$  for Run C, respectively. We have chosen parameters for the new runs such that after the onset of the plasmoid instability the current sheets would have widths (estimated from the scaling law  $\delta \sim \delta_{SP}(S_c/S)^{1/2}$ ) ranging from  $d_i$  (Run A) to  $4d_i$  (Run C). This is the parameter regime where we may expect to observe a transition from the “Hall reconnection triggered by plasmoids” regime to the “plasmoid-dominated reconnection” regime, depending on the ratio  $\delta/d_i$ . The initial condition and governing parameters for these runs allow a clear separation of length scales: the drivers of reconnection (the two merging islands) are on the largest scale  $\sim 1$ ; the initial current layer width  $\sim 0.01$ ; the Sweet-Parker width  $\sim 10^{-3}$ ; and the ion skin depth  $d_i \sim 1 - 4 \times 10^{-4}$ . Therefore, the simulations cover all distinct stages of reconnection from the initial current sheet thinning to the onset of plasmoid instability, which subsequently may or may not lead to onset of Hall reconnection.

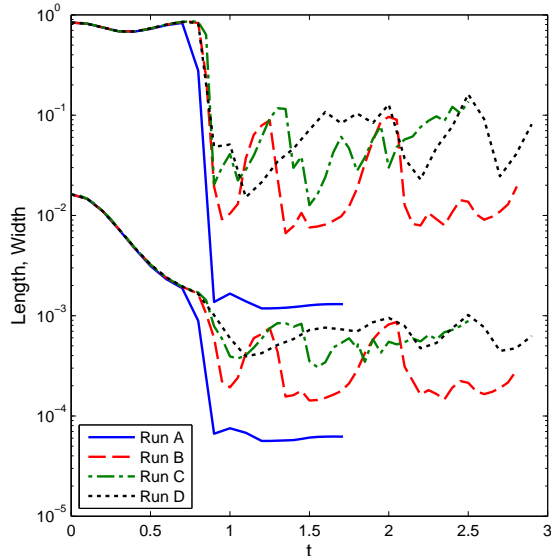


Figure 3: (Color online) The length (upper curve) and width (lower curve) of the main reconnection current sheet as a function of time, for four different runs.

### III. SIMULATION RESULTS

Our primary diagnostics are the reconnection rate and the length and width of the main reconnection current sheet. The reconnection rate is measured as the time derivative of the reconnected magnetic flux. In the presence of the plasmoid instability, usually there are more than one current sheets at a given instance. We define the main reconnection current sheet as the one located at where the two primary coalescing islands touch each other. This is the (generally unique) point where the separatrix flux surface bounding the two merging islands intersects itself. For example, in the second panel of Figure 5, the main reconnection current sheet is the one at the center, between  $x = 0$  and  $x = 0.1$ . The length and width are measured as the full width at quarter maximum.

Figure 2 shows the time history of the reconnection rate, and Figure 3 shows the time history of the length and width of the main reconnection current sheet, for four different runs. Initial current sheet thinning occurs from  $t = 0$  to  $t = 0.7$ . During this period, the four runs are very similar because the Hall current has yet to play an important role. The current sheet width thins from the initial  $\delta \sim 10^{-2}$  down to  $\delta \sim \delta_{SP} \sim 10^{-3}$ . Meanwhile, the reconnection rate gradually rises to  $3 \times 10^{-3}$ . The plasmoid instability sets in at approximately  $t = 0.7$ . Thereafter, the three new runs exhibit qualitatively different behaviors. In Run A, the



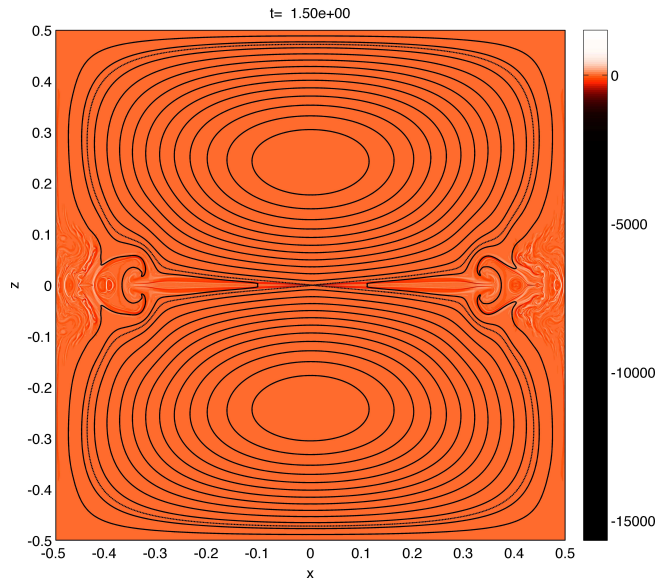


Figure 4: (Color online) Out-of-plane electric current density at  $t = 1.5$  for Run A, overlaid with magnetic field lines, in the whole simulation box. Dashed lines indicate separatrices, which are the field lines that separate the two merging islands.

plasmoid instability immediately triggers a strong onset of Hall reconnection, which expels all the plasmoids, and the system is left with a single X-point. After that, the system reaches a quasi-steady state with the reconnection rate and current sheet geometry approximately time-independent. This run gives the highest reconnection rate (up to 0.04) of the four runs, and the current sheet is also the shortest and narrowest. The aspect ratio (width/length) of the current sheet in the quasi-steady state is approximately  $1/20$ . Figure 4 shows the out-of-plane electric current density, overlaid with magnetic field lines, in the whole domain at  $t = 1.5$ . Dashed lines denote the separatrices which are the field lines that separate the two merging islands. The reconnection site clearly shows a Petschek-like geometry with the separatrices opening up in the downstream region.

In Run B (see Figure 5 for a few snapshots of the key stages), the plasmoid instability does not immediately lead to onset of Hall reconnection. An onset occurs at approximately  $t = 1.3$ , triggered by a new plasmoid formed in the main reconnection current sheet. Subsequently all plasmoids are wiped out. However, it appears that Hall reconnection with a single X-point is unstable for this set of parameters, and the system makes a transition back to an extended current sheet. The current sheet length reaches a maximum ( $\simeq 0.1 = 500d_i$ ) at  $t = 2$ , whereupon it becomes unstable again and breaks up into plasmoids. This second

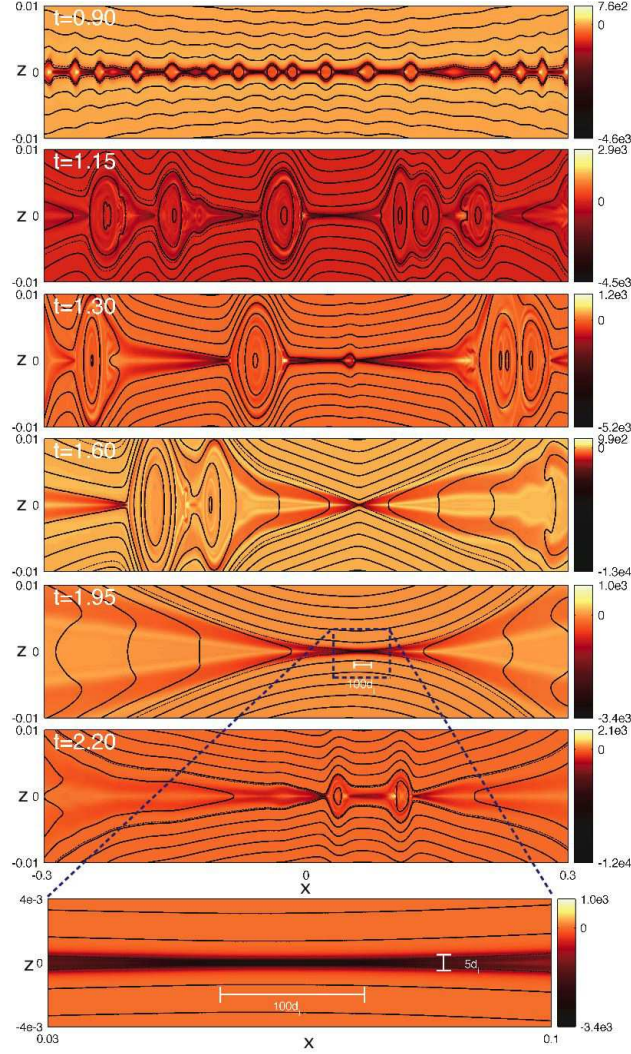


Figure 5: (Color online) Time sequence of the out-of-plane electric current density for Run B, overlaid with magnetic field lines. Dashed lines indicate separatrices. From top to bottom: (1) The Sweet-Parker current sheet breaks up into a chain of plasmoids. (2) The plasmoids grow in size; some of them are expelled to the downstream region; some of them coalesce to form larger plasmoids. (3) A new plasmoid forms at the main current sheet. (4) The formation of the new plasmoid leads to an onset of Hall reconnection that eventually expels all plasmoids. (5) The current sheet becomes extended again. (6) Subsequently, the extended current sheet breaks up into plasmoids, which lead to another onset of Hall reconnection. The bottom panel shows an expanded view of the extended current sheet at  $t = 1.95$  (enhanced online).

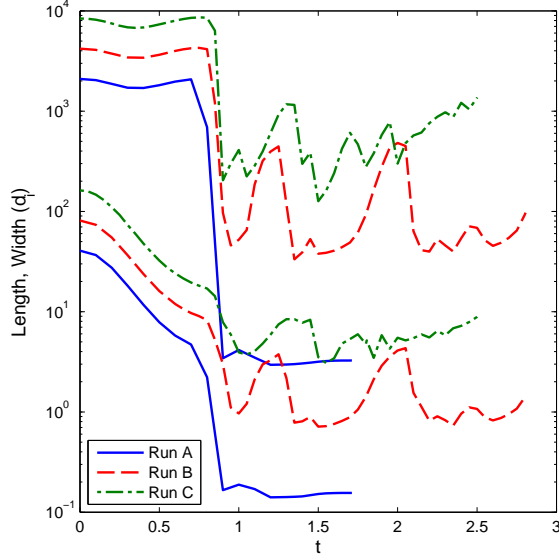


Figure 6: (Color online) The length (upper curve) and width (lower curve) of the main reconnection current sheet, normalized to the ion skin depth  $d_i$ , as a function of time for Run A to Run C.

onset of plasmoid instability leads to another onset of Hall reconnection, resulting in a single X-point again. Conceivably, this cycle will continue repeatedly until the system runs out of flux. Indeed, towards the end of this run, we observe that the length and width of the main current sheet start to rise again (Figure 3). In this regime, which we have called the intermediate regime, the system is caught in between Hall reconnection with a single X-point, and plasmoid-dominated reconnection with many X-points. The resulting reconnection rate shows a strong fluctuation between 0.005 to 0.03. For Run C, because  $d_i$  is well below the smallest scale caused by the plasmoid instability, the system never makes a transition to Hall reconnection. The reconnection rate from Run C, ranging from 0.005 to 0.013, is similar to that from Run D, which is a resistive MHD simulation ( $d_i = 0$ ).

In Figure 6 we replot the time histories of the length and width of the main current sheet as shown in Figure 3, but this time in units of  $d_i$ . Hall reconnection is characterized by the decoupling of ions and electrons at scales smaller than  $d_i$ , and the dissipation region where the frozen-in condition is broken is significantly smaller than the  $d_i$  scale. Run A clearly exhibit these features, as the current sheet width in quasi-steady phase is approximately  $0.15d_i$ . On the other hand, the main current sheet in Run B is never significantly thinner than  $d_i$ . The minimum current sheet width is approximately  $0.7d_i$  in this run. This suggests that the Hall reconnection after onset is not as robust as it is in Run A. The current sheet

width in Run C only reaches a minimum of approximately  $3d_i$ . That is why Run C never shows any onset of Hall reconnection.

#### IV. DISCUSSION

An important question is, why does Run B revert to an extended current sheet after the onset of Hall reconnection? To answer this question, it is important to appreciate that although the global Lundquist number  $S$  is high ( $S = 5 \times 10^5$ ) for these runs, the resistivity is not negligible on the length scale of  $d_i$ . The reason is that  $L/d_i$  is also a large number, which is often the case in many plasmas of interest. A relevant dimensionless parameter that quantifies how resistive the plasma is on the  $d_i$  scale is the Lundquist number based on  $d_i$ , defined as  $S_{d_i} \equiv V_A d_i / \eta$ . For Run A, B, and C, the Lundquist numbers based on  $d_i$  are 200, 100, and 50, respectively.

Recently, it has been suggested by Cassak *et al.* that over a certain range of  $S_{d_i}$ , resistive Hall reconnection exhibits bistability, *i.e.* both Sweet-Parker and Hall reconnection are physically realizable.[8, 20](Cassak *et al.* use the notation  $\eta'$ , which is  $1/S_{d_i}$ .) The condition for bistability may be expressed as[8]

$$\frac{L}{d_i} > S_{d_i} > S_{d_i}^c. \quad (5)$$

Here the condition  $L/d_i > S_{d_i}$  is equivalent to the condition  $\delta_{SP} > d_i$  for the existence of the Sweet-Parker solution, and the condition  $S_{d_i} > S_{d_i}^c$  simply means that the plasma cannot be too resistive on the  $d_i$  scale, otherwise the Hall solution will cease to exist. When  $S_{d_i}$  becomes lower than  $S_{d_i}^c$ , the system transitions back to Sweet-Parker reconnection. The critical value  $S_{d_i}^c$  is found to be approximately 50 in Ref. [8] for a double tearing mode configuration with two current sheets in a system of dimensions  $409.6d_i \times 204.8d_i$ . Also, electron inertia is included in that study, with a mass ratio  $m_e/m_i = 1/25$ . At this point, it is not clear how the critical value  $S_{d_i}^c$  may depend on the mass ratio, the plasma beta, the system size with respect to  $d_i$ , the global configuration, and boundary conditions. While these dependencies should be addressed in future work, we conjecture that  $S_{d_i}^c$  is a monotonically increasing function of  $L/d_i$  such that the condition  $L/d_i > S_{d_i}^c$  is always satisfied. (This leaves open the possibility that in the asymptotic limit  $L/d_i \rightarrow \infty$ , the critical value  $S_{d_i}^c$  may become independent of  $L/d_i$ .) We now discuss the numerical evidence in support of this conjecture.

Note that the inequality  $S_{d_i}^c > S_{d_i} > L/d_i$  is not possible, for if it were, both Sweet-Parker and Hall solutions would be unrealizable. We refer to this as a situation that leaves the system in deadlock, for which there is no numerical evidence. In fact, whenever the condition  $L/d_i > S_{d_i}$  is violated, the system will settle down to the Hall solution. This suggests that the critical value  $S_{d_i}^c$  will self-adjust so that the condition  $L/d_i > S_{d_i}^c$  is always satisfied. In the present study, it appears that Run B, with  $S_{d_i} = 100$ , is already below the critical value  $S_{d_i}^c$  for transition. (That implies that the critical value  $S_{d_i}^c$  is greater than 100, higher than approximately 50 found by Cassak *et al.* This is consistent with our conjecture that  $S_{d_i}^c$  may increase with  $L/d_i$ , as our system size is significantly larger. However, note that many other conditions in this study are significantly different from those employed by Cassak *et al.*, which could also account for the difference.) Therefore, a single X-point Hall reconnection geometry is not sustainable for this set of parameters. On the other hand, the other solution that the system will tend to make a transition to — the Sweet-Parker solution — is also unstable due to the plasmoid instability. Note that the present situation should be distinguished from the system deadlock discussed above. In the present situation, the Sweet-Parker solution should be realizable according to the bistability argument. It is the plasmoid instability, which is beyond the scope of the bistability theory as presently constructed, that makes the Sweet-Parker solution unrealizable.

When an onset of Hall reconnection is triggered by the plasmoid instability, the relevant length scale in the condition (5) is no longer the original Sweet-Parker current sheet length  $L$ , but the distance  $l$  between the two neighboring plasmoids that are next to the site of onset. The condition for transition back to the Sweet-Parker solution is now

$$\frac{l}{d_i} > S_{d_i}^c > S_{d_i}. \quad (6)$$

That implies the distance between two nearby plasmoids has to be at least  $100d_i$  for the transition to be possible in Run B. If we take into account that  $S_{d_i}^c$  may depend on  $l/d_i$ , the minimum requirement for  $l$  may be even larger. This explains why the transition back to the Sweet-Parker solution does not occur immediately after the onset.

To further verify that the Hall solution is unstable for the set of parameters of Run B, we carry out the following test. We take the solution of Run A at  $t = 1.3$  and restart with the ion skin depth  $d_i$  artificially lowered to  $2 \times 10^{-4}$ , the same value as Run B. Figure 7 shows the time sequence of this test. As a result of lowering  $d_i$ , the opening angle between

the separatrices quickly closes up, first starting from the center, then gradually propagating outward. The current sheet becomes extended at the same time and eventually breaks up into plasmoids. This test confirms that the Hall solution is indeed unsustainable for the set of parameters of Run B.

Recently, there has been controversy regarding whether the bistability demonstrated in Ref. [8] is due to electron inertia effects.[20–22] Run A in the present study may be interpreted as an independent verification of the claim made individually by Cassak *et al.* [20] and Sullivan *et al.* [22] that bistability survives even in the absence of electron inertia. In Run A, the Hall solution is realized and remains stable after onset of the plasmoid instability. However, the Sweet-Parker solution clearly exists, because the Sweet-Parker width  $\delta_{SP} \simeq 10^{-3}$  is significantly above the ion skin depth  $d_i = 4 \times 10^{-4}$ . Had it not been the intervention of the plasmoid instability, Run A would have realized the Sweet-Parker solution. Therefore, within the framework of the original bistability theory, where the plasmoid instability is not taken into account, both Sweet-Parker solution and Hall solution are realizable for the set of parameters of Run A, and the system is bistable. Now because of the plasmoid instability, the Sweet-Parker solution in Run A becomes physically unrealizable, and the Hall solution is the only possibility. The present study is valuable as an independent test of the phenomenon of bistability because it is done with a different code and a different initial condition. (Both Cassak *et al.* and Sullivan *et al.* use the code F3D.[23])

## V. CONCLUSION

Our results show that the transition to fast reconnection in large, high-Lundquist-number plasmas can be realized by the complex interplay between the plasmoid instability and Hall reconnection. We have clearly demonstrated that the plasmoid instability can facilitate the onset of Hall reconnection, in a regime where the Hall reconnection would otherwise remain inaccessible because the criterion  $d_i > \delta_{SP}$  is not met (Runs A and B). However, the onset of Hall reconnection does not always lead to a single X-point topology, with all plasmoids expelled. Run B demonstrates the possibility that a single X-point geometry is itself unstable, and after the onset of Hall reconnection, reverts to an extended current sheet of the type that led to an X-point in the first place. In this case, the reconnection is

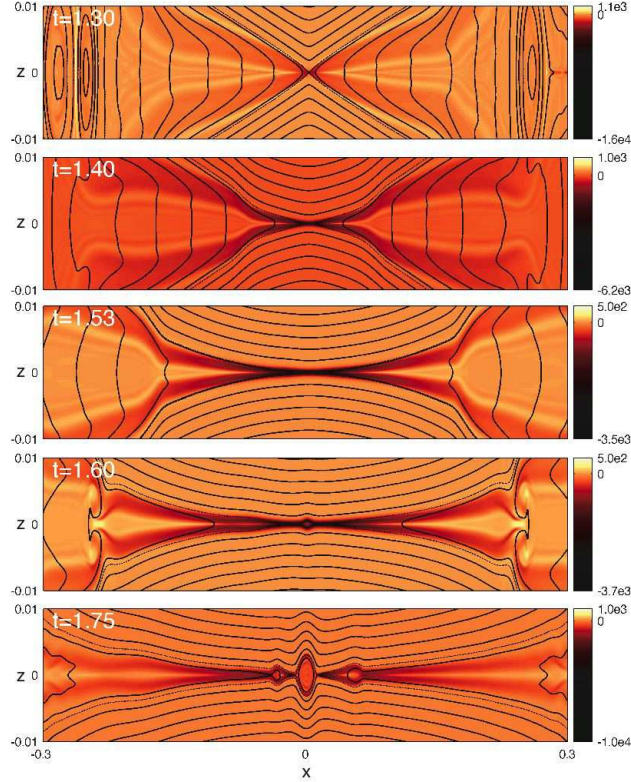


Figure 7: (Color online) Time sequence of the out-of-plane electric current density for the artificial test, overlaid with magnetic field lines. The initial condition is taken from Run A at  $t = 1.3$ , with the ion skin depth  $d_i$  artificially lowered from  $4 \times 10^{-4}$  to  $2 \times 10^{-4}$ , which is the same as Run B. The opening angle between the separatrices quickly closes up, first starting from the center, then gradually propagating outward. As the current sheet becomes extended, it becomes unstable to the plasmoid instability (enhanced online).

characterized by sporadic, bursty behavior with new plasmoids constantly being generated. Because of the intermittent onset of Hall reconnection, on average the reconnection rate is higher than it is when the plasmoid instability does not trigger Hall reconnection (Run C), but lower than it is when a robust Hall reconnection site forms (Run A).

The results presented here provide a possible resolution to a dichotomy in the existing literature — the X-point geometry in Hall reconnection[5, 6, 8], versus the extended current sheet geometry embedded with plasmoids in fully kinetic simulations[14]. Our results demonstrate that the dichotomy is false. We have shown that for some range of parameters (Run B) resistive Hall MHD allows the current sheet to become extended again after the onset, and subsequently new plasmoids are generated. That is not to say that Hall MHD

can be a satisfactory substitute for fully kinetic models. What we have demonstrated is that the single X-point topology is not inevitable even in the simplest resistive Hall MHD model if the system size is large enough, and in this respect, Hall MHD results for large systems bear a qualitative resemblance with those from fully kinetic models. The results presented here may be viewed as a first step towards implementing more sophisticated closures in the generalized Ohm's law, which may enable fluid models to represent key kinetic effects in reconnection simulations. Fully kinetic simulations of large systems, such as the Earth's magnetosphere or the solar atmosphere, with realistic physical parameters are likely to remain computationally too expensive even in the near-future era of exascale computing. In this respect, our results represent a useful point of departure towards the goal of representing kinetic effects in the global modeling of laboratory, space, and astrophysical plasmas.

### Acknowledgments

This work is supported by the Department of Energy, Grant No. DE-FG02-07ER46372, under the auspice of the Center for Integrated Computation and Analysis of Reconnection and Turbulence (CICART), the National Science Foundation, Grant No. PHY-0215581 (PFC: Center for Magnetic Self-Organization in Laboratory and Astrophysical Plasmas), NASA Grant Nos. NNX09AJ86G and NNX10AC04G, and NSF Grant Nos. ATM-0802727, ATM-090315 and AGS-0962698. YMH is partially supported by a NASA sub-contract to the Smithsonian Astrophysical Observatory's Center of Astrophysics, Grant No. NNM07AA02C. Computations were performed on facilities at National Energy Research Scientific Computing Center. YMH would like to thank Dr. Naoki Bessho for commenting on an earlier version of the paper.

- 
- [1] E. G. Zweibel and M. Yamada, *Annu. Rev. Astron. Astrophys.* **47**, 291 (2009).
  - [2] A. Bhattacharjee, Z. W. Ma, and X. Wang, *Phys. Plasmas* **8**, 1829–1839 (2001).
  - [3] P. A. Sweet, *Nuovo Cimento Suppl. Ser. X* **8**, 188 (1958).
  - [4] E. N. Parker, *Astrophys. J. Suppl.* **8**, 177–211 (1963).
  - [5] Z. W. Ma and A. Bhattacharjee, *Geophys. Res. Lett.* **23**, 1673–1676 (1996).
  - [6] J. C. Dorelli and J. Birn, *Geophys. Res.* **108**, 1133 (2003).



- [7] A. Bhattacharjee, *Annu. Rev. Astron. Astrophys.* **42** 365-384 (2004).
- [8] P. A. Cassak, M. A. Shay, and J. F. Drake, *PRL* **95**, 235002 (2005).
- [9] M. Yamada, Y. Ren, H. Ji, J. Breslau, S. Gerhardt, R. Kulsrud, and A. Kuritsyn, *Phys. Plasmas* **13**, 052119 (2006).
- [10] N. F. Loureiro, A. A. Schekochihin, and S. C. Cowley, *Phys. Plasmas* **14**, 100703 (2007).
- [11] B. Coppi, E. Galvao, R. Pellat, M. N. Rosenbluth, and P. H. Rutherford, *Sov. J. Plasma Phys.* **2**, 533 (1976).
- [12] A. Bhattacharjee, Y.-M. Huang, H. Yang, and B. Rogers, *Phys. Plasmas* **16**, 112102 (2009).
- [13] Y.-M. Huang and A. Bhattacharjee, *Phys. Plasmas* **17**, 062104 (2010).
- [14] W. Daughton, V. Roytershteyn, B. J. Albright, H. Karimabadi, L. Yin, and K. J. Bowers, *PRL* **103**, 065004 (2009).
- [15] P. A. Cassak, M. A. Shay, and J. F. Drake, *Phys. Plasmas* **16**, 120702 (2009).
- [16] L. S. Shepherd and P. A. Cassak, *PRL* **105**, 015004 (2010).
- [17] P. N. Guzdar, J. F. Drake, D. McCarthy, A. B. Hassam, and C. S. Liu, *Phys. Fluids B* **5**, 3712 (1993).
- [18] S. Gottlieb, C.-W. Shu, and E. Tadmor, *SIAM Rev.* **43**, 89 (2001).
- [19] R. J. Spiteri and S. J. Ruuth, *SIAM J. Numer. Anal.* **40**, 469 (2002).
- [20] P. A. Cassak, M. A. Shay, and J. F. Drake, *Phys. Plasmas* **17**, 062105 (2010).
- [21] A. Zocco, L. Chacón, and A. N. Simakov, *Phys. Plasmas* **16**, 110703 (2009).
- [22] B. P. Sullivan, A. Bhattacharjee, and Y.-M. Huang, “On the question of hysteresis in Hall MHD reconnection,” *Phys. Plasmas* (submitted).
- [23] M. A. Shay, J. F. Drake, M. Swisdak, and B. N. Rogers, *Phys. Plasmas*, **11**, 2199 (2004).